CWC20 NAU Technical Design Report
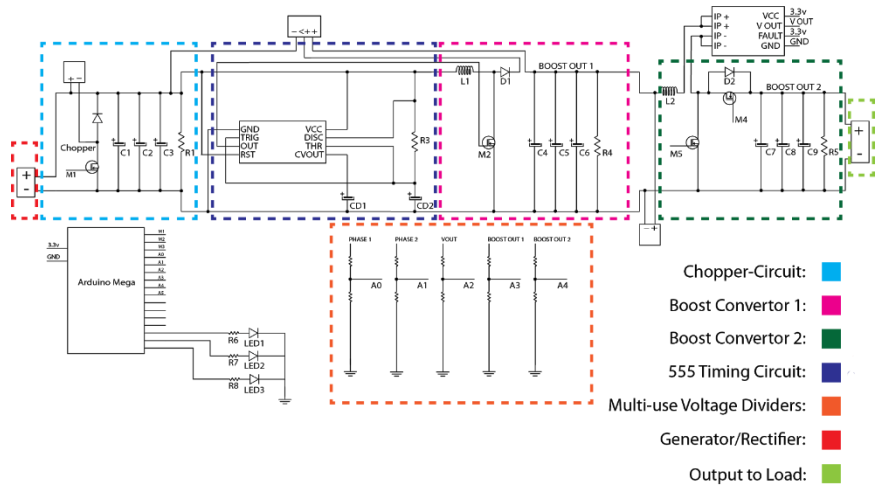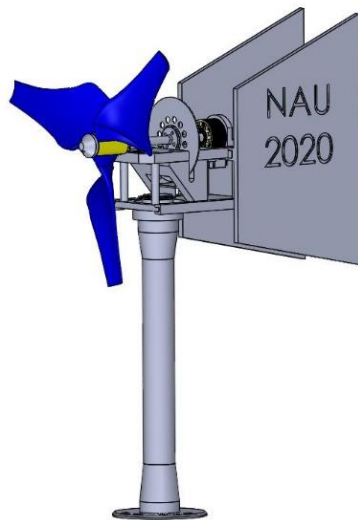
Student Authors:

Member	Role	Contact
Lucas Duncan	ME Team Lead	ldd55@nau.edu
Calum Eikenberry	EE Auxiliary Team Lead	cje223@nau.edu
Nigel Grey	EE DC-DC Convertor Team Lead	ng474@nau.edu
Ethan Maltaverne	ME budget liaison/ Motor specialist	epm49@nau.edu
Daniel Massaglia	ME Manufacturing Member	dm976@nau.edu
Marina McCue	ME Aerodynamics Lead	marina_mccue@nau.edu
Matt Mennell	ME Manufacturing Lead	mlm636@nau.edu
Sean Veden	ME Brake Design Lead	jfv32@nau.edu

Table of Contents

List of Table

List of Figures

Executive Summary (Sean)

The Northern Arizona University (NAU) Collegiate Wind Competition (CWC) 2020 turbine team completed a design for a small-scale wind turbine. The turbine is a three-blade design with a passive yaw, dynamic and mechanical braking, and a closed-loop controlled synchronous boost converter electrical subsystem. The parts used in this turbine were either commercially available or manufactured by the team. The design team was split into three: one mechanical engineering team and two electrical engineering teams. The mechanical engineering team was tasked with designing the aerodynamic, structural, and mechanical parts of the turbine. The electrical DC-DC converter team was tasked with the design and simulation of the converter topology. The electrical auxiliary team was tasked with converting the DC-DC team's design into a printed circuit board (PCB) and complimenting it with low forward-voltage component selections. To aid in the design process, the team used computer programs such as MATLAB-Simulink, QBlade, Arduino IDE, and SolidWorks. Once the parts were designed, testing was completed to ensure the design worked as expected. The testing procedures are described within this document.
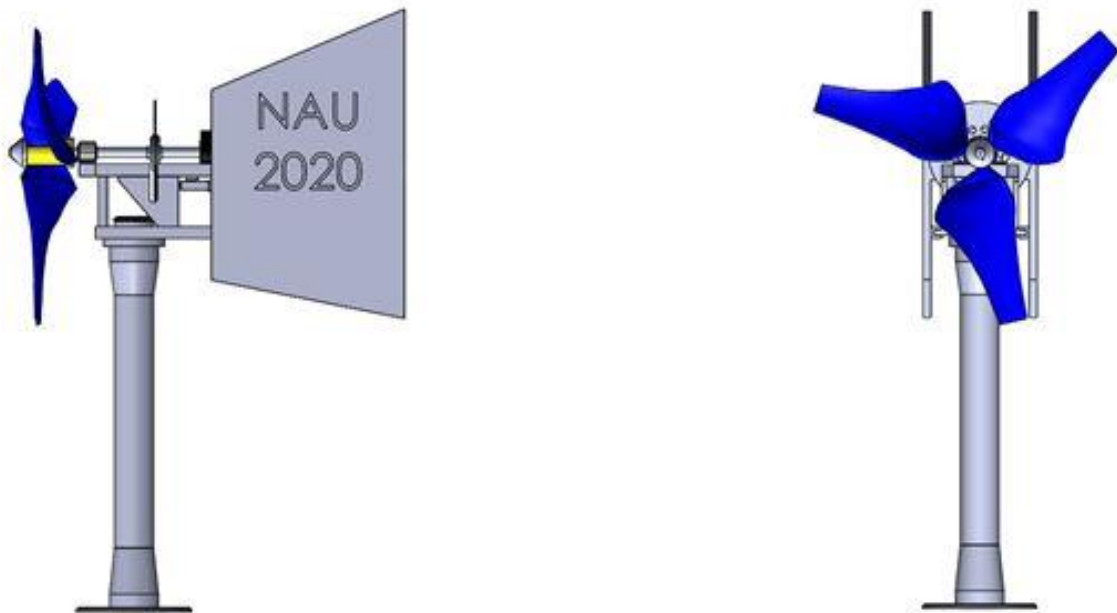
Figure 1: Full Assembly

1. Design Requirements (Ethan)

Table 1: Design Requirements [1]

Electrical Engineering Requirements	Mechanical Engineering Requirements
Voltage must be direct current (DC) and less than 48 V at any point in the system	Withstand wind speeds up to 22 m/s during operation and up to 25 m/s during braking
No capacitors greater than 10 J of energy storage may be used on the turbine side of the system	Yaw rate of 180 °/s
Capacitors and inductors may not be used as bulk energy storage on the turbine side of PCC	Cut-in between 2.5 m/s and 5 m/s wind speeds
All external wired connections must be optically isolated	+/- 10 % maximum average power
Team load must run on a maximum of 120 VAC	Control rated power between 12 m/s and 18 m/s wind speeds
Electrical systems are tied to ground at 100 kΩ or lower resistor	Braking system activated when an emergency stop button is pressed, disconnected from PCC, or subjected to wind speeds greater than 22 m/s

Our design revolved primarily around the predetermined engineering requirements. This gave the team a direction for which to start searching for hardware. The first mechanical engineering requirement was the ability to withstand 25m/s wind speed. This led us to develop a ridged tower to minimize deflection. A 2-in wide tower tube stock with a wall thickness of 0.5-in was selected to be lathed to the proper fitment for the receiving bearing chosen for the lower nacelle. the yaw rate restriction drove us to balance and center all internal nacelle parts to further enable the influence of the yaw that was yet to be developed. The earliest possible cut-in speed was one of our top priorities in blade development. The target was cut in at 2.5 m/s. this meant both blade development and motor selection had to be focused on this characteristic. After the cogging torque testing of 3 motors, we were able to find a motor with power rating above 100 W at 4,000 RPM and the least resistive torque of any motor tested. blades were reiteratively altered to find the most aggressive blade without compromising the performance in the windspeeds up to 25 m/s.

Our brake system would need to have several times the braking forces of previous models due to the runaway test. This led our design to utilize a 135 mm disk and an 80 N actuator to accomplish a total braking force of 5.4Nm. The team produced a reverse mounted drop-down brake system that allowed the brake disk to intrude into the lower nacelle cabin area, ultimately solving this performance issue.

Throughout this project appropriate mounting and dimensioning was found to be one of the most crucial aspects of development. With our extremely compact design most components found themselves within 3 mm of each other. This constraint pushed us to develop the multipurpose rail system implemented into the upper nacelle plate. This system utilizes the limited space of the nacelle and maintains assembly simplicity and reducing required hardware.

2. Static Performance Analysis (Marina)

The wind turbine blades were first designed using MATLAB, analyzed and modified using QBlade, and then rendered using SolidWorks. The MATLAB code assumed an ideal rotor with wake rotation and calculated chord length and twist angle from a design tip speed ratio of 1.5, angle of attack of 16 degrees, rotor radius of 20.6 cm, hub radius of 1.9 cm, and 3 blades. This information, along with selected airfoils, were inputted into QBlade and the power performance was analyzed. Chord length and twist angle were exaggerated, and different airfoils were analyzed until desirable characteristics were achieved. The final blade geometry is located below in Table 2. Figure 2 displays the coefficient of power versus tip speed ratio for angular velocities ranging from 0 to 3500 RPM, with a maximum coefficient of power of 0.3 at the design tip speed ratio.

Table 2: Wind Turbine Blade Geometry

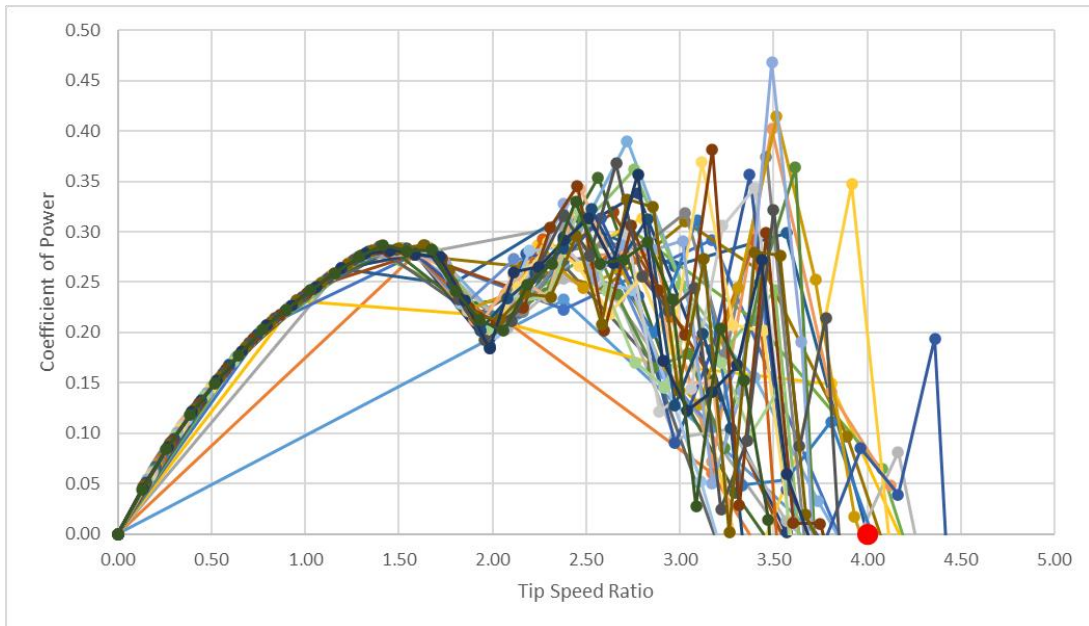| Local Rotor Radius (cm)	Chord Length (cm)	Twist Angle (Degrees)
1.7	10.0	45
3.4	10.8	27
5.2	11.2	18
6.9	9.1	13
8.6	7.6	9.0
10.3	6.5	6.5
12.0	5.6	4.7
13.7	4.9	3.3
15.5	4.5	2.2
17.2	4.0	1.3
18.9	3.7	0.6
20.6	3.4	0

Figure 2: Coefficient of Power versus Tip Speed Ratio

The wind turbine cuts-in at 2.0 m/s and produces a rated power of 28 W at 11 m/s, shown in the power curve below in Figure 3. Using the power curve and a Rayleigh probability distribution, the annual energy production was calculated and is displayed in Figure 4.
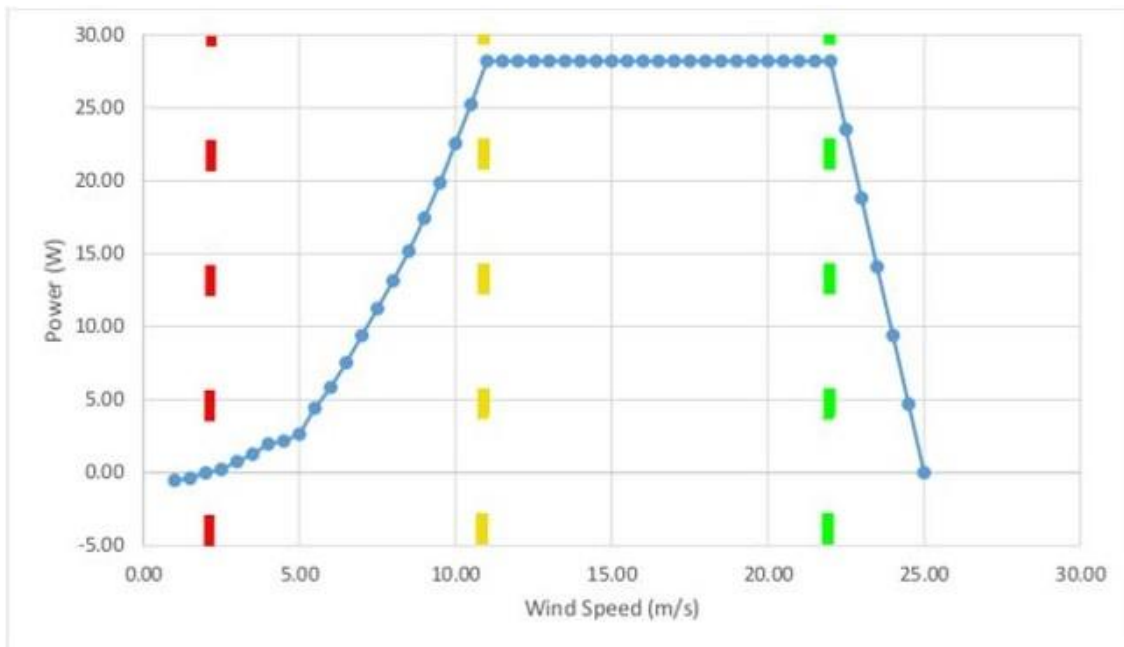
Figure 3: Aerodynamic Power Curve
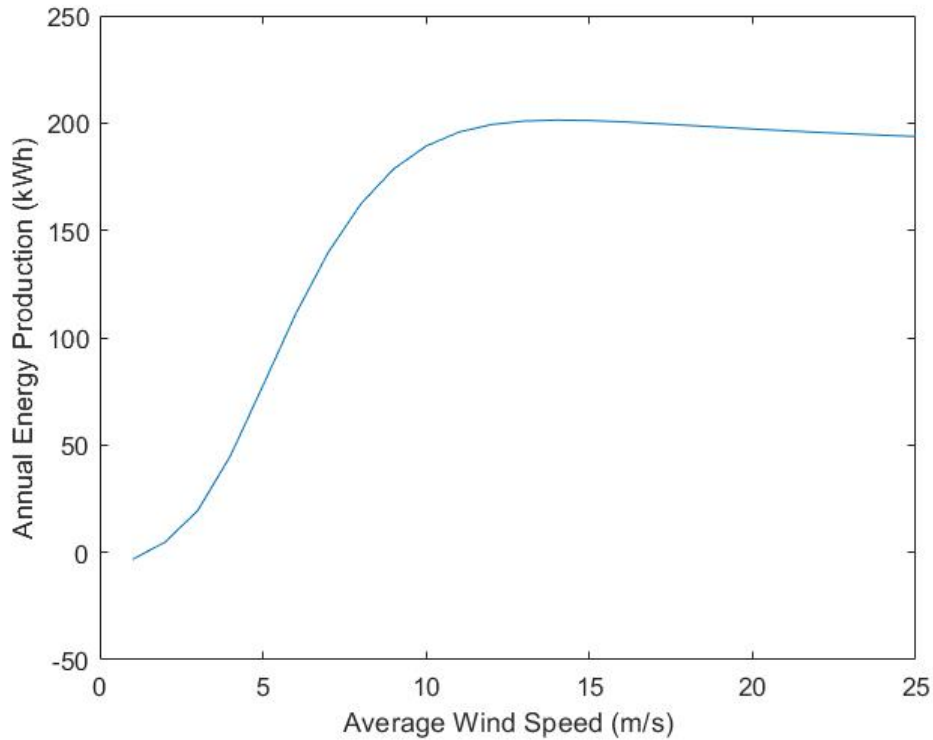
Figure 4: Annual Energy Production

3. Mechanical Loads Analysis

Table 3: Mechanical Component Factor of Safety (FOS)

System	Material(s)	Load Description	Loads Applied	Minimum FOS
Blades	Polycarbonate	Thrust, Centrifugal	$T = 17.0\ N$ $\Omega = 4341\ RPM$	2.74

3.1. Blade Analysis (Marina)

The final wind turbine blade finite element analysis was conducted using SolidWorks, shown below in Figure 5. The centrifugal load was determined from the runaway rotor speed, which was calculated using the tip speed ratio where the coefficient of power is zero (see the red dot from Figure 2) about 4.0, rotor radius of 20.6 cm, and maximum wind speed of 25 m/s. The thrust force was calculated using air density for standard atmospheric conditions 1.225 $\mathrm{kg/m^3}$, area of the rotor plane, maximum wind speed, and ideal axial induction factor of one third. In the next iteration of the FEA, the lift and drag force would be calculated to determine the resultant force along each section of the blade. This would then be used in lieu of the estimated thrust force.

Figure 5: Wind Turbine Blade Finite Element Analysis

3.2. Shaft Analysis (Matt)

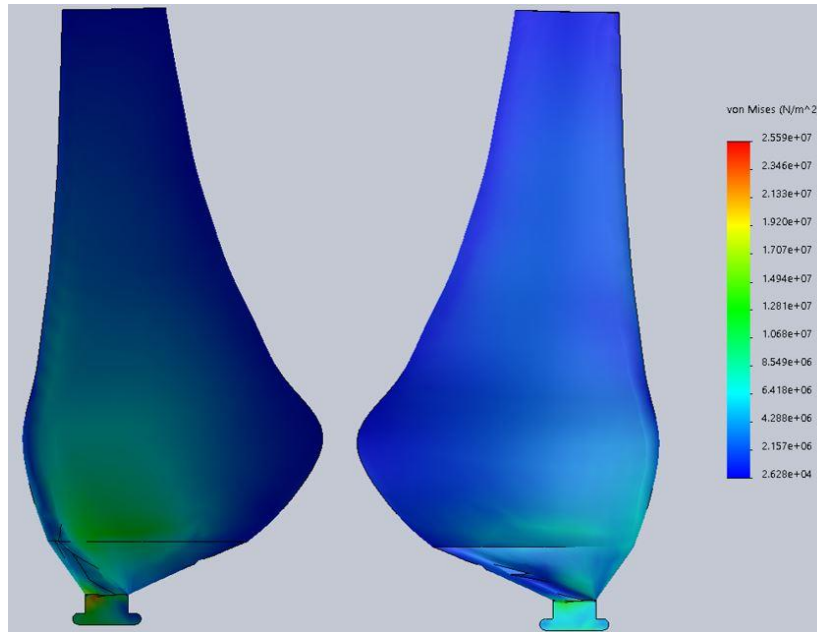The shaft design, in Figure 6, relies on dimensions such as length and cross-sectional areas as well as the maximum centripetal forces experienced. These forces can be determined by the startup torque and during hard braking. The chosen design includes a short section of the shaft which is has a larger diameter and milled to have a key shape in order to lock the disc in rotation. One end of the shaft is attached to a coupler to the motor shaft. The other end of the shaft is turned down over two inches with an inch of threads cut out. This allows the hub to slide onto the shaft and lock rotation when the hub nose screws on to clamp the hub in place. The shaft is locked in place through the motor mount while support for the weight of the hub and blades on one end and reduced friction is helped with the use of a pillow block bearing mounted to the top nacelle. Due to incompletion of manufacturing of final shaft no physical testing was taken but through calculations a factor of safety of 2.1 was determined.
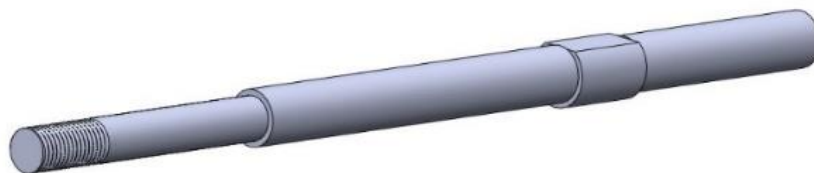
Figure 6: Shaft

3.3. Brake Analysis (Sean)

Figure 7 above shows the brake assembly within the upper level nacelle plate and provides a label of parts shown. The slider and the rail system used is made of polycarbonate and is 3D printed. The braking slider and stopper behind the disk have a slot where a brake pad is pressed into each. The braking slider is fastened to the linear actuator to clamp the brake disk when the actuator is extended. The linear actuator

shown is controlled using an Arduino microcontroller and a linear actuator control board. The control board allowed for less coding and allows for fine tuning of the actuator speed and stroke length.

Figure 7: Brake Assembly

Based the on analysis of the blades, the torque that must be overcome to stop the rotation of the blades is shown in Table 4 below. This table outlines the torque produced by the blades at runaway wind speeds and the factor of safety the braking system.

Table 4: Runaway Wind Speeds and Braking System Factor of Safety

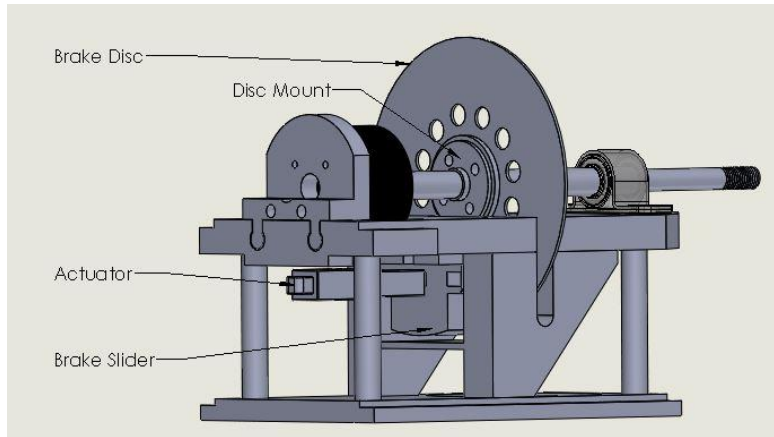| Wind Speed [m/s]	Torque of Blades [N-m]	Factor of Safety
18	2.5	2
22	4	1.35
25	5	1.08

The brake disk is 67.5 mm in radius and the linear actuator produces 80 Newtons which means the torque of the braking system is 5.4 N-m. The design decision to make the disk 135 mm in diameter was to ensure that the sub-system could achieve a FOS of 2 at runaway speeds. Since runaway speed testing begins at 18 m/s, the design will need to actuate at the beginning of the speed ramp up for the safety of the turbine. If testing was able to have been completed the team may have found that this design was over engineered and in that case the size of the disk could be modified. The 80N actuator was chosen based on estimated values of tip speed ratio and power produced by the blades at runaway speeds. These values led to back of the envelope calculations that told the team that an 80N actuator would be the safest option. The L12P actuator used produces the maximum force sold in the micro size. For this reason, the only viable option to modify the torque of the braking system was to change the brake disk size. This design can stop the turbine with the use of a push button and with speed sensors that actuate the braking system when runaway wind speeds are sensed.

3.4. Nacelle Analysis (Daniel)
The nacelle is comprised of two sections including a lower and upper plate. The lower plate, made of aluminum manufactured in the NAU machine shop, lets wiring from the generator and brake assembly run down the tower while not binding when the turbine experiences direction change. The upper nacelle

plate is produced from the Rapid Lab using polycarbonate material. It is made up of two sections that bolt to the bottom plate which are both designed to fasten the nacelle cover and yaw in place.

The top nacelle plate serves multiple purposes. Starting with the bottom of the top plate, an actuator mounts for the brake to linearly push a brake pad against the brake rotor housed within the nacelle. Moving to the upper face, a single pillow block with a pressed bearing provides support to the drive shaft. In addition to this block, the generator itself helps provide support through a coupler where the shaft ends. The generator mounts to a motor mount which utilizes a rail system to mount into the upper nacelle.

3.5. Tower Analysis (Daniel)

Using steel tube stock to manufacture, the tower of the turbine was designed on SolidWorks and used in a stress and displacement analysis. In order to machine the tube stock to a desired shape, a 2-inch outer diameter with a half inch wall thickness was utilized for ideal dimensions. It is important to make sure that the tower design could withstand the forces it would experience in the wind tunnel. Shown in **Error! Reference source not found.** and Figure 9, the von Mises stress distribution and stress analysis across the chosen tower design. The importance of these stresses relates to where a part can fail due to fatigue or yielding. Using mild steel, the amount of stress that the tower is miniscule in respect to what it would take to yield the steel. Computing a factor of safety of 116, the towers wall thickness could be decreased from $1/4^{th}$ of an inch to $1/8^{th}$ of an inch and still have a large factor of safety.

Figure 9: Von Mises Tower Analysis   Figure 8: Tower Stress Analysis
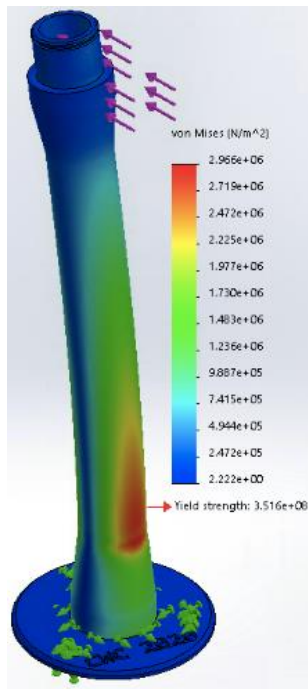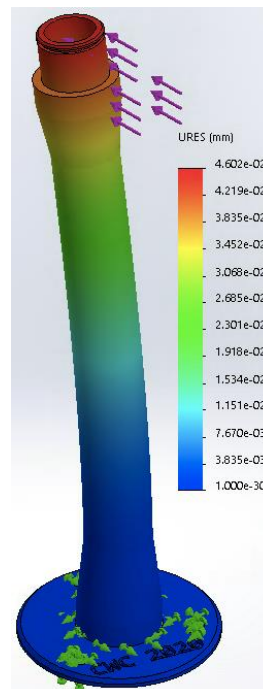
Error! Reference source not found. illustrates that the yield strength of the tower is 3.5e8 Pa, and the maximum stress that the tower would experience at maximum wind load was estimated to be 3e6 Pa. Using mild steel for material selection, it can be concluded that this material and dimensions have more than enough strength to withstand the expected forces.

4. Yaw System (Lucas & Marina)

The Yaw of the turbine helps keep the rotor plane perpendicular to air flow as it sits on a ball bearing. This design utilizes two tails to increase the surface area which decreases the amount of force needed to hold the nacelle in an ideal position. Attached rails with fasteners to secure the yaw to the nacelle.
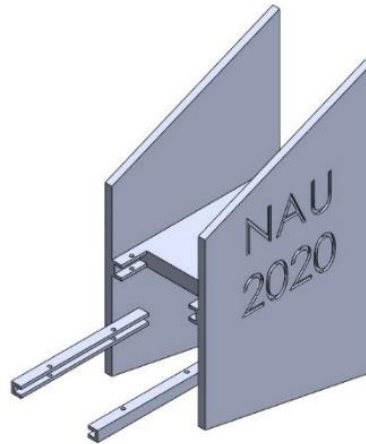

Figure 10: Yaw
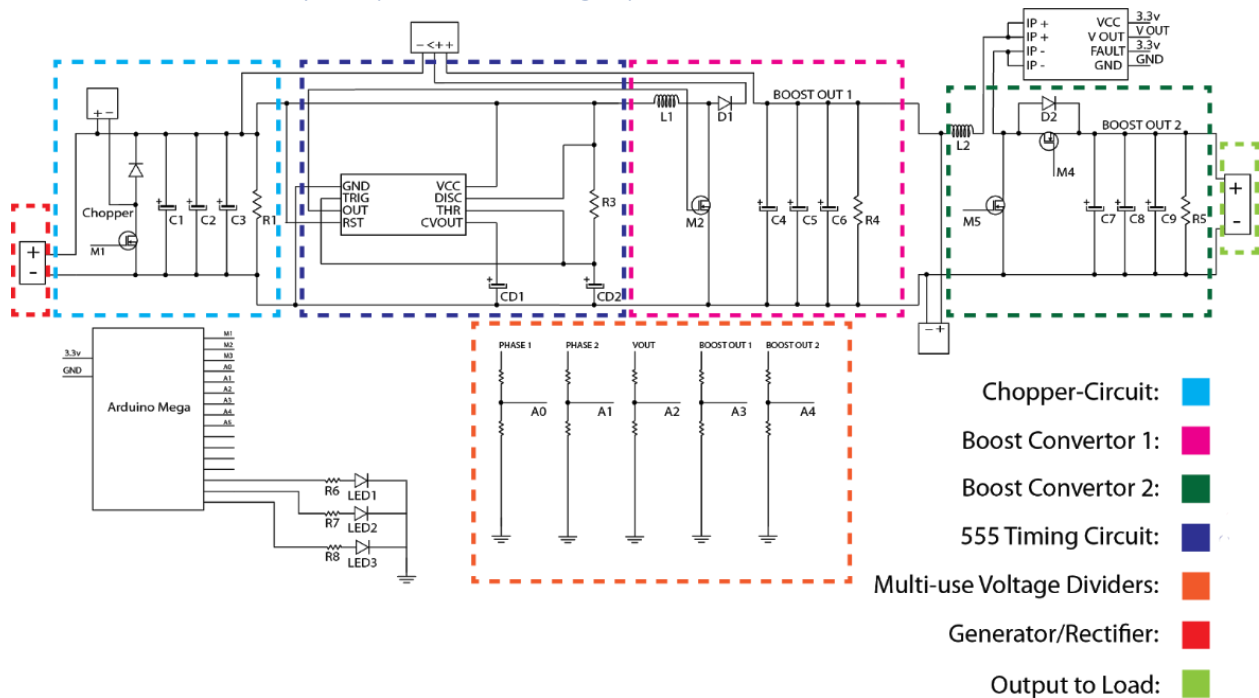
5. Electrical Analysis (Calum & Nigel)

Figure 11: Greater-than-one-line Diagram

The electrical analysis and sub-system design processes were delegated to two sub-teams: the DC-DC team and the Auxiliary team.
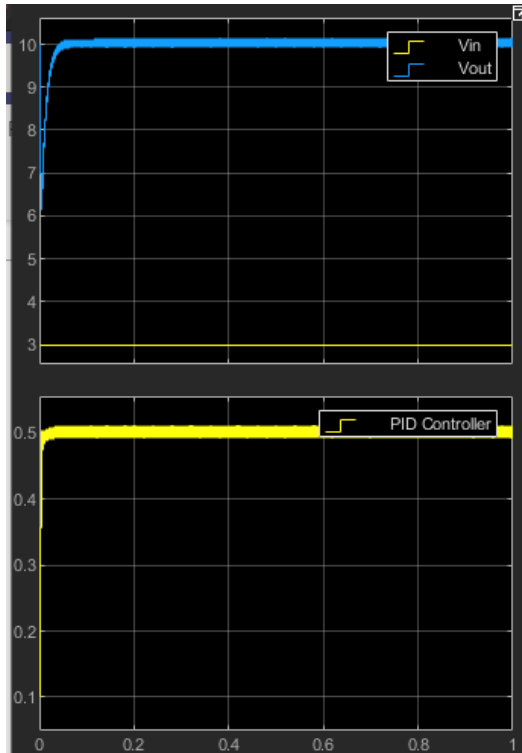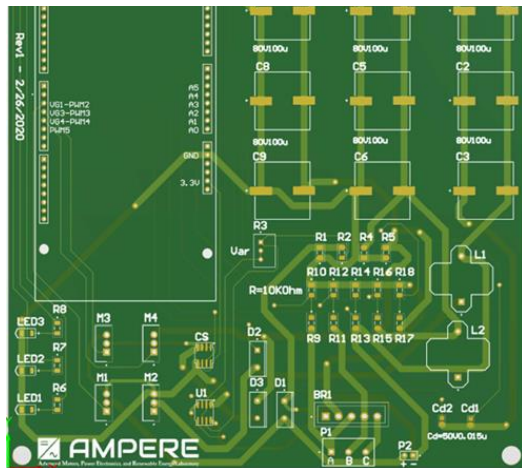
Figure 12: Simulink Duty Cycle Output

The **DC-DC team** primarily worked to design, simulate, and build a three-stage boost convertor system that utilized a synchronous boost converter topology (two complementary MOSEFTs) in place of a standard MOSFET and diode combination (*see Figure 11*). The goal of the design was to maximize power generation at low wind speeds, while minimizing the total voltage drop of the system (*see Figure 11*). Most testing for the synchronous topology was done with a MATLAB-Simulink PID simulation that returned exactly a 3.3x voltage output with little ripple current (*see Figure 12).* This operation was repeated with breadboarding to similar results. Difficulty was expected upon implementing this design within the overall circuit due to several parallel processes running independently on the Arduino, and so an optional diode was implemented to provide a non-synchronous topology option.

Figure 13: Final PCB Design

The **Auxiliary team** worked in parallel with the DC-DC team to optimize all electrical components (i.e. rectifier, auxiliary component wiring, generator) to best complement the low cut-in design and synchronous topology. In addition, the Auxiliary team spearheaded the printed circuit board (PCB) design and construction (*see Figure 13*), which integrated the entire power/control system from Figure 13 into one circuit. Furthermore, the team tested multiple control algorithm's functionality with an Arduino Uno which provided successful operations of necessary breaking functions. until hard programming was deemed unnecessary due to the ability to flash programs directly from MATLAB-Simulink.

Altium Designer was utilized by the Auxiliary team to create a 6" by 6", single-sided PCB (*see Figure 13)* with all discrete components mounted to it (excluding braking chopper chassis mount resistor and packaged boost convertor for initial microcontroller power source). The design of this PCB included LEDs to allow visual verification that each stage (rectifier, first boost converter, second boost converter) was on, flush-mounted spacing for the Arduino Mega, additional footprints for parallel capacitors for quick changes in signal rectification after each convertor, and the maximum separation of control components/routing from power components/routing as to minimize signal interference. The control components lay along the bottom-left of the board and the power components across the top-right to center-right.
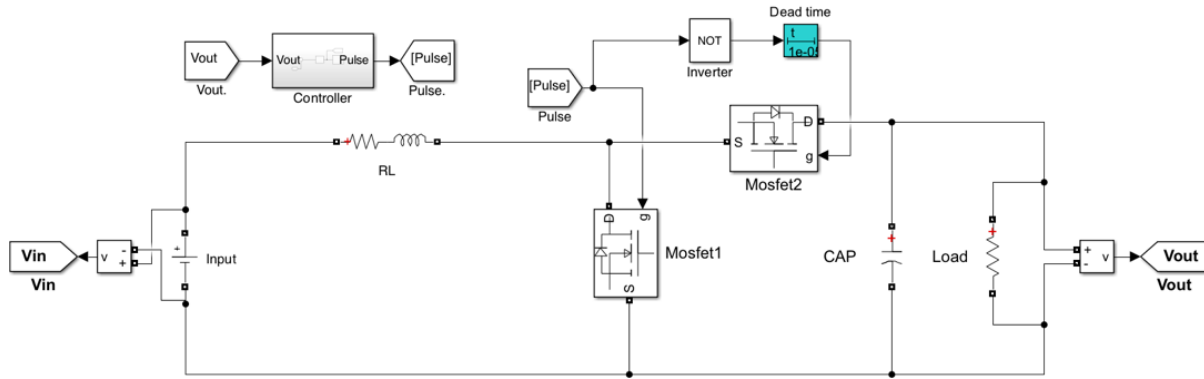
Figure 14: PI-Controlled Synchronous Boost Converter Schematic

The intended load attached at the end of the schematic diagram (***see Figure 11***) was to be a fixed resistance load with a 300W power rating and 10 Ohm resistance. Upon further testing the team would home in on the optimal resistance/power rating.

6. Software Description, System Control (Calum & Nigel)

MATLAB Simulink was used for circuit and closed-loop control simulations (***see Figure 14***). Simulink also allowed for a block-programming style that easily modularized the numerous electrical and mechanical turbine control algorithms and allowed a direct export to the Arduino Mega microcontroller (***see Figure 15***).
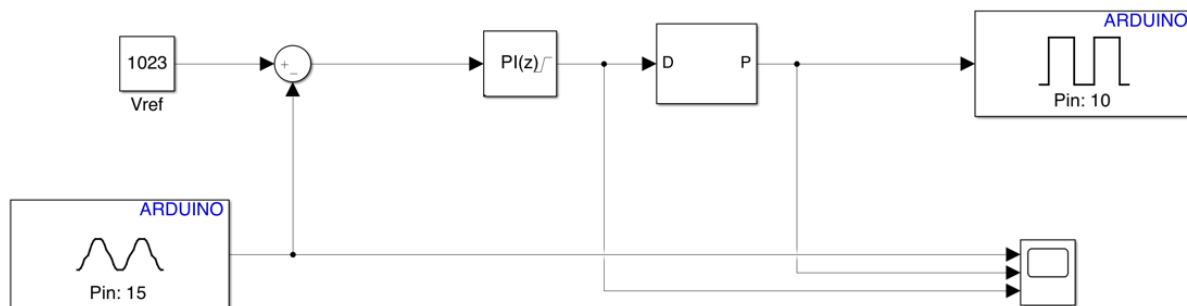

Figure 15: PI-Controller Arduino Program

All control modules (***see Figure 16***), were to be modeled within the Simulink environment and then exported directly to the microcontroller (same style of programming implemented in Figure 14) to reduce timing complications and optimize the controller's multithreading capability.

Control Module Descriptions:

1. Dump-Load Circuit: when an overspeed event occurs, route the rectified signal through an external resistor to ground via the ***"Chopper Circuit"*** in Figure 11. This control module is active only during the ***"Durability Task Power Dump"*** region (***see Figure 16)***.
2. Phase 1-2 Voltage Measurement: calculate the turbine rpm via phase 1 and 2 x-axis crossing point difference. This module occurs as soon as the microcontroller is powered on as to detect the point in time to trigger the system brake for the ***"Initiate Brake"*** region (***see Figure 16***).

3. PI Controller: utilizes proportional integral calculation to control second stage boost converter duty-cycle.
4. Current Sensor Measurement: used to detect and signal if load is disconnected. This module is active as soon as the "System Cut-In Region" is reached and detects the *"Disconnect from Load"* region (***see Figure 16***).
5. Stage 2, 3, & 4 Voltage Measurements: voltage divider circuits used to detect electrical potential at each key stage; trigger LEDs to provide visual feedback. This is also utilized to detect the *"Disconnect from Load"* region (***see Figure 16***).
6. Actuator Signal: provides PWM signal for mechanical braking control and is utilized during the *"Initiate Brake"* region (***see Figure 16***).
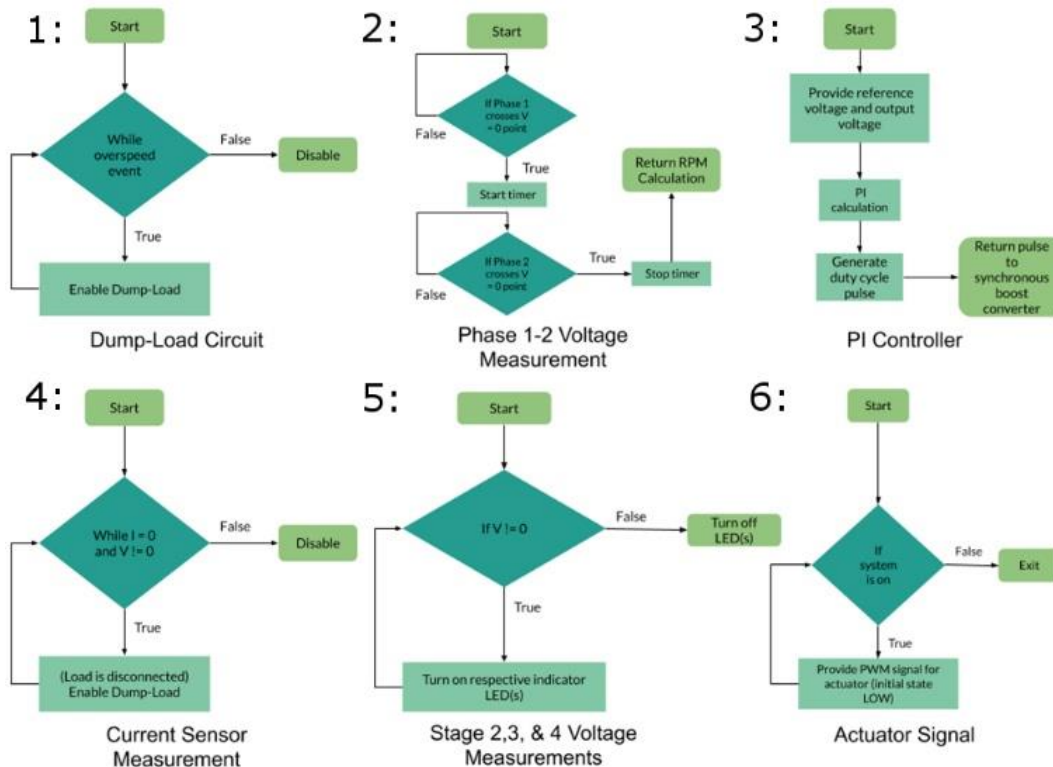

Figure 16: Control Module Flowcharts

7. Testing Results

7.1. Electrical Testing Procedure (Calum & Nigel)

Testing and power quality measurements of the PCB with all soldered components was to take place immediately after receiving of the PCB from the manufacturer if the project were able to continue. LEDs were integrated after each stage of conversion within the circuit to provide visual feedback to the tester, and an oscilloscope would be used to provide exact measurements per the CWC2020 rules and requirements. The design (***see Figure 11)*** featured the ability to change the capacitance values to decrease noise and increase signal integrity. Due to the modular capacitance and closed-loop control, additional filtering techniques would not likely be needed. The generator output would be tracked with the use of a dynamometer throughout this testing.

7.2. Mechanical Testing Procedure

The testing procedures for the turbine have come to a stop, but in the following sections each major sub-system testing procedures that have been done will be discussed. The findings during these tests will be gone over and how it aided in the team's design decisions. Also discussed below is the testing procedures that would have taken place if the times would allow.

7.2.1. Blades & Hub (Lucas & Matt)

The blades and hub subsystem were tested early during the semester. Members of the team assembled a safety container out of wood and Plexiglass, shown in Figure 18. Attached to the back of the box was a rail system which fastened a motor in place to turn a shaft up to 3300 rpm, shown in Figure 17. The box is equipped with two self-aligning flange bearings which helped smooth un-concentric rotation. The rotor testing taken concluded with two sets of broken blades which had different density values. It was found that the area where the blades formed into a key for the hub was the weakest point. This led to a redesign of the hub and blades to fix the failure point and another rotor strength test was conducted, which was successful. The results of the rotor strength test are displayed below in Table 5.
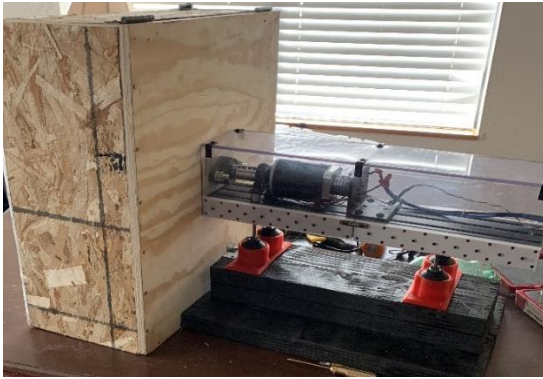

Figure 17: Rotor Strength Test Enclosure

Figure 18: Blades in Enclosure

Table 5: Rotor Strength Test Results

Rotor Iteration	Material	Fill	Failure
1st	ABS	10%	Yes, 2200 RPM
1st	ABS	20%	Yes, 3000 RPM
2nd	ABS	100%	No

7.2.2. Tower/Baseplate/Nacelle (Daniel)

Improper design relating to these systems of the turbine can cause catastrophic failure within operation. Failures can include the tower disconnecting from the baseplate due to faulty welds, improper bearing fitment resulting in a low preforming yaw, and overall shearing of the tower due to shear forces. Shown above (**See Figure 8**), the tower analysis gave reassurance that a final design could withstand possible forces up to ten times the maximum amount of yield stress experienced. Once the tower and baseplate are manufactured, testing by mounting the turbine to a car to simulate wind would determine if the math

behind the design was correct. Forces experienced can be estimated with a known temperature and speed of travel.

7.2.3. Brake (Sean)

Figure 19: Actuator Slider Testing

The braking system for the turbine was one aspect of the assembly that was behind schedule. Due to this, the testing of the sub-system was not completed before the project was halted. The Arduino code and circuit were built, and the actuator was able to be controlled with the use of a push button (**See Figure 19**). The plan was to analyze the braking sub-system through physical testing, using an apparatus made to simulate the loads produced by the blades of the turbine. Through this testing, the material of the brake pads and the proper stroke and speed of the linear actuator would have been chosen. Since the factor of safety for the braking system is below the industry standard of 2 at max runaway speed of 25m/s, the braking system would need to be actuated during the ramp up phase at 18 m/s. This would require further testing to ensure that the sensing system used in the design could detect wind speeds of 18 m/s and actuate the actuator promptly.

7.2.4. Yaw (Lucas, Marina & Matt)

The yaw system was another subsystem that was put on the back burner while other subsystem was being completed. The plan was to 3D print the Yaw for the final assembly after spring break. Yaw would be tested via car testing with the final assembly. The team made a mount to attach to roof rack that would secure the turbine to car. The team would force the turbine to rotate through turns and high wind speeds. The teams most concern was making sure yaw's rail system did not shear. The team would experiment with different 3D print fills and try to test for shear points and fatigue life.

7.2.5. Shaft (Lucas, Marina & Matt)

The shaft subsystem testing was on hold until the brake system was completed. The teams main concerned was shearing while braking the turbine. The shaft would be tested via caring testing. The team would stop the turbine at various wind speeds and applied brake forces. It was determined through blade tests our shaft and the startup torque of the motor in use.

References

[1] National Renewable Energy Laboratory, "US Department of Energy Collegiate Wind Competition 2020," 2019.